[Autophagy 5:5, 625-635; 1 July 2009]; ©2009 Landes Bioscience

Research Paper

Identification of *Atg5*-dependent transcriptional changes and increases in mitochondrial mass in *Atg5*-deficient T lymphocytes

Linda M. Stephenson,[1,†] Brian C. Miller,[1,†] Aylwin Ng,[3] Jason Eisenberg,[3] Zijiang Zhao,[1] Ken Cadwell,[1] Daniel B. Graham,[1] Noboru N. Mizushima,[4,5] Ramnik Xavier,[3] Herbert W. Virgin[1,2] and Wojciech Swat[1,*]

[1]Department of Pathology and Immunology; [2]Department of Molecular Microbiology; Washington University School of Medicine; St. Louis, Missouri USA; [3]Center for Computational and Integrative Biology; Massachusetts General Hospital; Harvard Medical School; Boston, Massachusetts USA; [4]Department of Physiology and Cell Biology; Tokyo Medical and Dental University; Tokyo, Japan; [5]Solution Oriented Research for Science and Technology; Japan Science and Technology Agency; Kawaguchi, Japan

[†]These authors contributed equally to this work.

Key words: T cells, cell differentiation and development, transgenic/knockout mice, ATG5, mitochondria

Autophagy is implicated in many functions of mammalian cells such as organelle recycling, survival and differentiation, and is essential for the maintenance of T and B lymphocytes. Here, we demonstrate that autophagy is a constitutive process during T cell development. Deletion of the essential autophagy genes *Atg5* or *Atg7* in T cells resulted in decreased thymocyte and peripheral T cell numbers, and *Atg5*-deficient T cells had a decrease in cell survival. We employed functional-genetic and integrative computational analyses to elucidate specific functions of the autophagic process in developing T-lineage lymphocytes. Our whole-genome transcriptional profiling identified a set of 699 genes differentially expressed in *Atg5*-deficient and *Atg5*-sufficient thymocytes (*Atg5*-dependent gene set). Strikingly, the *Atg5*-dependent gene set was dramatically enriched in genes encoding proteins associated with the mitochondrion. In support of a role for autophagy in mitochondrial maintenance in T lineage cells, the deletion of *Atg5* led to increased mitochondrial mass in peripheral T cells. We also observed a correlation between mitochondrial mass and Annexin-V staining in peripheral T cells. We propose that autophagy is critical for mitochondrial maintenance and T cell survival. We speculate that, similar to its role in yeast or mammalian liver cells, autophagy is required in T cells for the removal of damaged or aging mitochondria and that this contributes to the cell death of autophagy-deficient T cells.

Introduction

Macroautophagy (herein autophagy) is a multistep process by which portions of cytoplasm and/or organelles are sequestered in a double membrane structure (autophagosome) and delivered to lysosomes for degradation.[1] Autophagy has been implicated in many cellular functions, including cell survival during starvation and stress, cell death and cellular differentiation.[1,2] However, the factors that determine whether the induction of autophagy contributes to cell survival or cell death in specific cell types are incompletely understood.[3] The molecular mechanism of autophagosome formation is evolutionarily conserved and requires two ubiquitin-like conjugation systems. One system generates conjugates of the proteins ATG5 and ATG12, which associate with ATG16 and are essential for elongation of the isolation membrane.[1,4] The ATG5-ATG12 conjugate has E3 ubiquitin ligase-like activity for the second ubiquitin-like system, the ATG8 (LC3) conjugation system.[5] The second system results in the formation of LC3 conjugated to phosphatidylethanolamine (LC3-II), which can be readily differentiated from unconjugated LC3 (LC3-I) based on their electrophoretic mobilities.[1] Both systems require the enzyme ATG7, which has E1-like activity.[4] Mice deficient in either of the autophagy genes *Atg5* or *Atg7* die in the first day after birth.[6,7]

Autophagy plays a critical role in the development and survival of lymphocytes. It has been reported that autophagy contributes to cell death in T cells after growth factor withdrawal.[8] Additional studies suggest that autophagy is an important death pathway in T cells lacking FADD activity, caspase-8 or Irgm-1.[9,10] However, other studies show that deletion of the autophagy gene *Atg5* results in decreased survival of T lymphocytes.[11] A similar result is observed in B-1a B cells when *Atg5* is deleted in B cells,[12] suggesting that autophagy plays a critical survival role in specific subsets of lymphoid cells. In addition, this process is also required in thymic epithelial cells for normal MHC-II peptide presentation and thymocyte selection.[13] Because autophagy and autophagy genes have many different roles in regulating the cellular environment, it is unclear how autophagy promotes lymphocyte survival.

One function of autophagy is the degradation of organelles to maintain cellular homeostasis.[14,15] Many recent studies have suggested that autophagy is important in the maintenance of mitochondria. Deletion of autophagy genes in yeast or murine

*Correspondence to: Wojciech Swat; Department of Pathology and Immunology; Washington University; 660 S. Euclid Ave; Box 8118; St. Louis, Missouri 63110 USA; Tel.: 314.747.8889; Fax: 314.362.1403; Email: swat@wustl.edu

Submitted: 02/05/09; Accepted: 02/10/09

Previously published online as an *Autophagy* E-publication: http://www.landesbioscience.com/journals/autophagy/article/8133

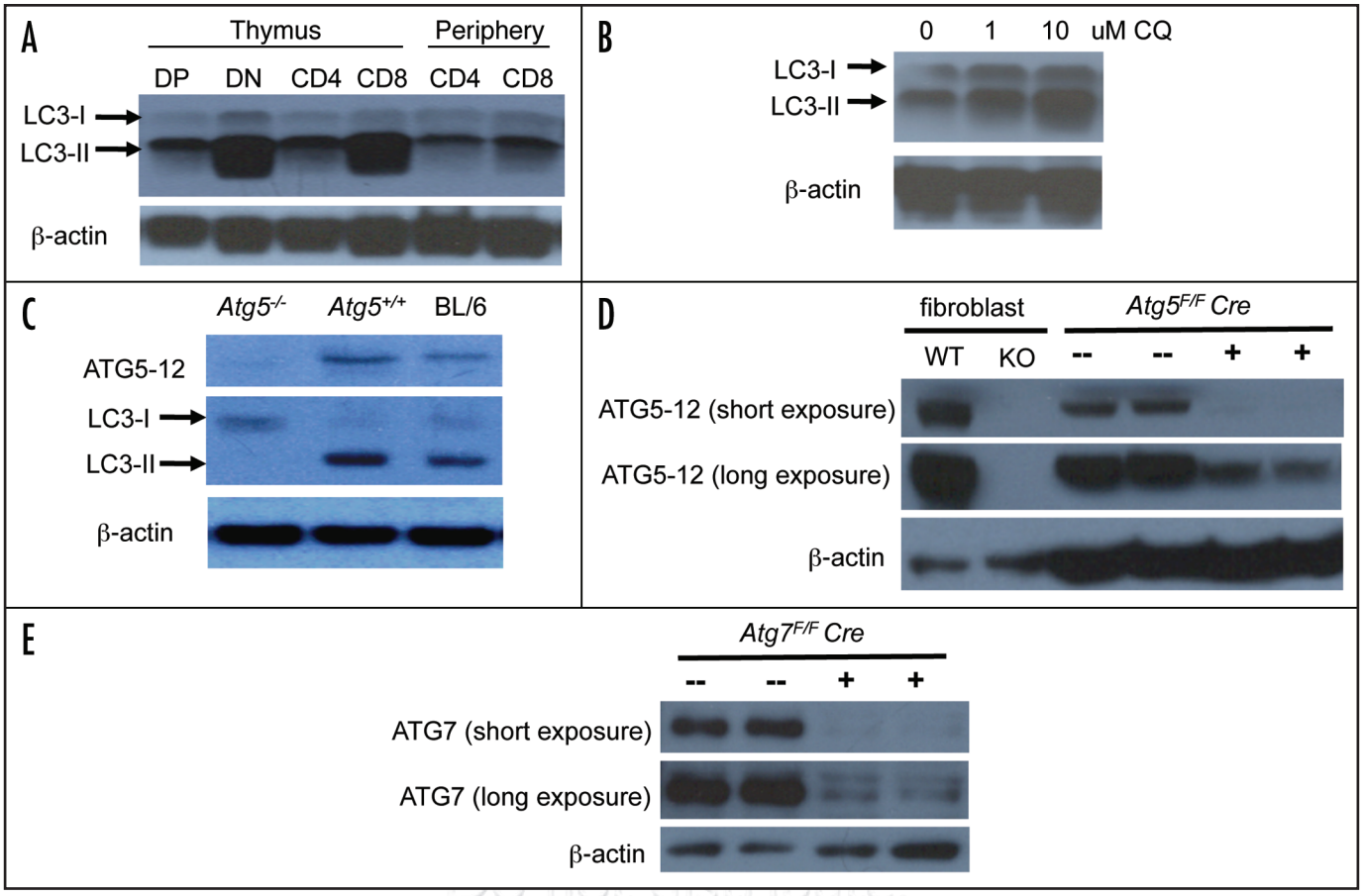

Figure 1. Constitutive autophagy in all subsets of wild-type T cells. (A) Lysates from FACS-sorted C57BL/6 thymus cells and MACS-bead sorted peripheral T cells were probed with antibodies against LC3 and β-actin. Representative blot from four independent experiments shown. (B) Lysates from C57BL/6 thymocytes cultured for 4 hours with the indicated concentrations of chloroquine were probed with antibodies against LC3 and β-actin. Representative blot from three independent experiments shown. (C) Lysates from *Atg5*$^{+/+}$ or *Atg5*$^{-/-}$ chimeras or C57BL/6 control thymocytes were probed with antibodies against ATG5, LC3 or β-actin. Representative blot from two independent experiments shown. (D) Lysates from *Atg5*$^{+/+}$ and *Atg5*$^{-/-}$ SV40-transformed murine embryonic fibroblasts and from *Atg5*$^{F/F}$ *Cre*$^{+}$ and *Atg5*$^{F/F}$ *Cre*$^{-}$ thymocytes were probed with antibodies against ATG5 and β-actin. Representative blot from three independent experiments shown. (E) Lysates from *Atg7*$^{F/F}$ *Cre*$^{+}$ and *Atg7*$^{F/F}$ *Cre*$^{-}$ thymocytes were probed with antibodies against ATG7 and β-actin. Representative blot from two independent experiments shown.

liver, β-islet cells, embryonic fibroblasts or macrophages results in the accumulation of damaged mitochondria.[7,16-18] Similarly, inhibition of autophagy in mammalian fibroblasts leads to increased mitochondrial mass.[19,20] Finally, imaging studies have revealed that opening of the mitochondrial permeability transition pore induces autophagy and the subsequent degradation of depolarized mitochondria.[21,22] Together, these studies indicate that autophagy is important for the clearance of damaged mitochondria, which accumulate in the absence of autophagy and can cause alterations in cellular biology.

Here we use three different approaches to study the role of autophagy in T cells in vivo. We demonstrate that autophagy is a constitutive process in developing and mature T cells and that *Atg5* and *Atg7* are required for thymocyte development and peripheral T cell homeostasis. Using *Atg5*-deficient T cells and integrative computational analysis, we identify a thymocyte-specific transcriptional signature associated with deficiency of *Atg5* in T cells and provide evidence that *Atg5* is required for the survival and mitochondrial maintenance of peripheral T cells.

Results

***Atg5* and *Atg7* are required for the maintenance of developing and mature T lymphocytes.** As a first step to understand the role of autophagy in T cells, we measured the levels of LC3-II as one marker of autophagic activity in developing and mature T lineage cells. We sorted thymic and peripheral T lineage subsets and probed the lysates with anti-LC3 antibodies. We observed robust LC3-II bands in all T cell subsets, indicating that autophagy is an active process in all stages of T cell development (Fig. 1A). To confirm that autophagy is an ongoing process in T cells, we cultured thymoyctes for 4 hours in the presence of increasing concentrations of chloroquine. Chloroquine results in an accumulation of LC3-II in actively autophagic cells.[23,24] As expected, LC3-II levels increased in a chloroquine dose-dependent manner (Fig. 1B), indicating that autophagy was ongoing in these cells.

Recent reports indicate that the autophagy gene *Atg5* is essential for normal T cell homeostasis,[11] however the mechanism by which *Atg5* controls T cell survival and/or proliferation remains unknown.

Table 1 **Loss of T cells in *Atg5*$^{-/-}$, *Atg5*$^{F/F}$ *Cre*$^{+}$ and *Atg7*$^{F/F}$ *Cre*$^{+}$ mice**

	Atg5 $^{+/+}$	*Atg5* $^{-/-}$	p value	*Atg5*$^{F/F}$ *Cre*$^{-}$	*Atg5*$^{F/F}$ *Cre*$^{+}$	p value	*Atg7*$^{F/F}$ *Cre*$^{-}$	*Atg7*$^{F/F}$ *Cre*$^{+}$	p value
Thymus	160.9 ± 9.9 (n = 41)	66.8 ± 8.0 (n = 44)	p < 0.0001	165.0 ± 12.2 (n = 25)	108.7 ± 9.1 (n = 29)	p = 0.0004	155.1 ± 19.8 (n = 8)	89.8 ± 11.6 (n = 9)	p = 0.0104
Lymph Nodes									
CD4^{+}	13.6 ± 0.9 (n = 34)	1.3 ± 0.3 (n = 37)	p < 0.0001	9.1 ± 0.9 (n = 16)	4.3 ± 1.0 (n = 20)	p = 0.0011	7.5 ± 1.5 (n = 7)	2.3 ± 0.4 (n = 7)	p = 0.0056
CD8^{+}	7.5 ± 0.6 (n = 34)	0.9 ± 0.6 (n = 37)	p < 0.0001	5.6 ± 0.6 (n = 16)	2.1 ± 0.6 (n = 20)	p = 0.0005	5.1 ± 1.1 (n = 7)	0.6 ± 0.1 (n = 7)	p = 0.0020
Spleen									
CD4^{+}	8.1 ± 0.6 (n = 37)	1.7 ± 0.2 (n = 41)	p < 0.0001	10.4 ± 4.3 (n = 20)	4.3 ± 0.6 (n = 24)	p < 0.0001	6.2 ± 0.9 (n = 7)	3.6 ± 0.7 (n = 7)	p = 0.0366
CD8^{+}	4.0 ± 0.3 (n = 37)	2.5 ± 0.4 (n = 41)	p = 0.0031	6.2 ± 0.6 (n = 20)	3.6 ± 0.4 (n = 24)	p = 0.0012	4.7 ± 0.8 (n = 7)	1.0 ± 0.3 (n = 7)	p = 0.0012

Data are mean ± SEM and represent multiples of 10^6 cells. The number of mice per group is indicated in parentheses. Chimera mice were analyzed between 6 and 13 weeks post-reconstitution. *Atg5*$^{F/F}$ *Cre* mice were analyzed between 6 and 13 weeks of age. *Atg7*$^{F/F}$ *Cre* mice were analyzed between 8 and 14 weeks of age.

To address these issues, we generated two different mouse models to delete *Atg5* in T cells. First, we used recombination activating gene (*Rag*)-1-deficient complementation[11,12,25] with E15.5-18.5 fetal liver cells from *Atg5*$^{-/-}$ or *Atg5*$^{+/+}$ embryos.[6] We note that mice reconstituted with *Atg5*$^{-/-}$ fetal liver cells have decreased viability compared with *Atg5*$^{+/+}$ reconstituted control mice (Supp. Fig. 1), however surviving young adult chimera mice appear generally healthy, permitting analysis of T cell development in this model. As an alternative approach, we generated *Atg5*-deficient T cells by breeding mice with conditionally targeted (floxed) *Atg5*[26] alleles to lck-*Cre* transgenics (*Atg5*$^{F/F}$ *Cre*$^{+}$). In these experiments, *Atg5*$^{F/F}$ *Cre*$^{-}$ mice were used as controls.

We first confirmed that T cells from these two mouse systems lack the ATG5 protein. Thymocyte lysates from *Atg5*$^{-/-}$ chimeras showed no detectable ATG5 protein expression (Fig. 1C). We also were unable to detect LC3-II (Fig. 1C), indicating that autophagy is abrogated in the absence of ATG5 in T cells. ATG5 levels were also reduced in *Atg5*$^{F/F}$ *Cre*$^{+}$ thymocytes (Fig. 1D), however residual levels of the protein were still detectable upon overexposure of the membrane, in spite of efficient recombination of the *Atg5*^{Flox} locus in thymocytes from *Atg5*$^{F/F}$ *Cre*$^{+}$ mice (Supp. Fig. 2).

We next analyzed the in vivo phenotype of *Atg5*-deficient T cells. In agreement with a previously published report,[11] thymus cellularity of *Atg5*-deficient chimeric mice analyzed between 6 and 13 weeks post fetal liver transfer was decreased approximately 2.4-fold compared to controls (Table 1), although there were no discernable alterations in the percentages of DN, DP, CD4^{+} SP and CD8^{+} SP (Fig. 2). Moreover, both the percentages and total numbers of CD4^{+} and CD8^{+} T cells in the lymph nodes and spleens of *Atg5*$^{-/-}$ chimeric mice were decreased compared to *Atg5*$^{+/+}$ chimeras (Fig. 2 and Table 1). A similar reduction in total numbers of thymocytes and peripheral T cells was observed in *Atg5*$^{F/F}$ *Cre*$^{+}$ mice compared to littermate controls (Fig. 2 and Table 1). We conclude that the decrease in T cell numbers is a result of T cell-intrinsic effects of the loss of *Atg5*.

It is possible that other functions of *Atg5* apart from its role in autophagy[27-29] may contribute to the phenotypic abnormalities of *Atg5*-deficient T cells. To address this issue, we deleted *Atg7*, another essential autophagy gene, from T cells using a conditional knockout approach similar to the one used above. We bred mice with conditionally targeted (floxed) *Atg7*[7] alleles to lck-*Cre* transgenics (*Atg7*$^{F/F}$ *Cre*$^{+}$). We observed reduced expression of ATG7 in *Atg7*$^{F/F}$ *Cre*$^{+}$ thymocytes by western blot analysis (Fig. 1E). Similar to *Atg5*$^{-/-}$ chimeras and *Atg5*$^{F/F}$ *Cre*$^{+}$ mice, total thymocytes and peripheral CD4^{+} and CD8^{+} T cell numbers were also reduced in *Atg7*$^{F/F}$ *Cre*$^{+}$ mice (Fig. 2 and Table 1). Together these data indicate that autophagy is required for the maintenance of both developing and peripheral T lymphocytes.

A role for *Atg5* in mitochondrial maintenance revealed by integrative computational analysis of whole-genome datasets. To obtain further insights into the functional pathways and networks through which autophagy maintains the T cell compartment, we developed an analytical framework that integrates gene expression analyses of wild-type and *Atg5*$^{-/-}$ thymocytes from chimeric mice with diverse information extracted from various genomic screens and databases including Gene Ontology (GO)[30] for functional classification, HPRD[31] for molecular interactions, HomoloGene[32] for homology mapping of genes, and NCBI PubMed and MILANO for literature co-citation analyses.[32,33] Whole-genome transcriptional profiling of *Atg5*$^{-/-}$ and *Atg5*$^{+/+}$ thymocytes identified a set of 699 differentially expressed genes (of which 259 genes were upregulated and 440 downregulated in *Atg5*$^{-/-}$ thymocytes, as compared to wild-type thymocytes) (Fig. 3A), permitting us to explore functional clusters within the set of differentially expressed genes and identify putative pathways and networks relevant to *Atg5* function in the T lymphoid lineage.

To ascertain whether the *Atg5*-dependent gene set was statistically enriched for genes implicated in subcellular compartment-associated processes, we first analyzed their annotations in Gene Ontology (GO) cellular component categories. Strikingly, the *Atg5*-dependent gene set was dramatically enriched in genes encoding proteins associated with the mitochondrion ($p = 3.7 \times 10^{-4}$) and nucleus ($p = 1.6 \times 10^{-4}$) (Fig. 3B). The mitochondrion GO signature was particularly interesting given the suggested

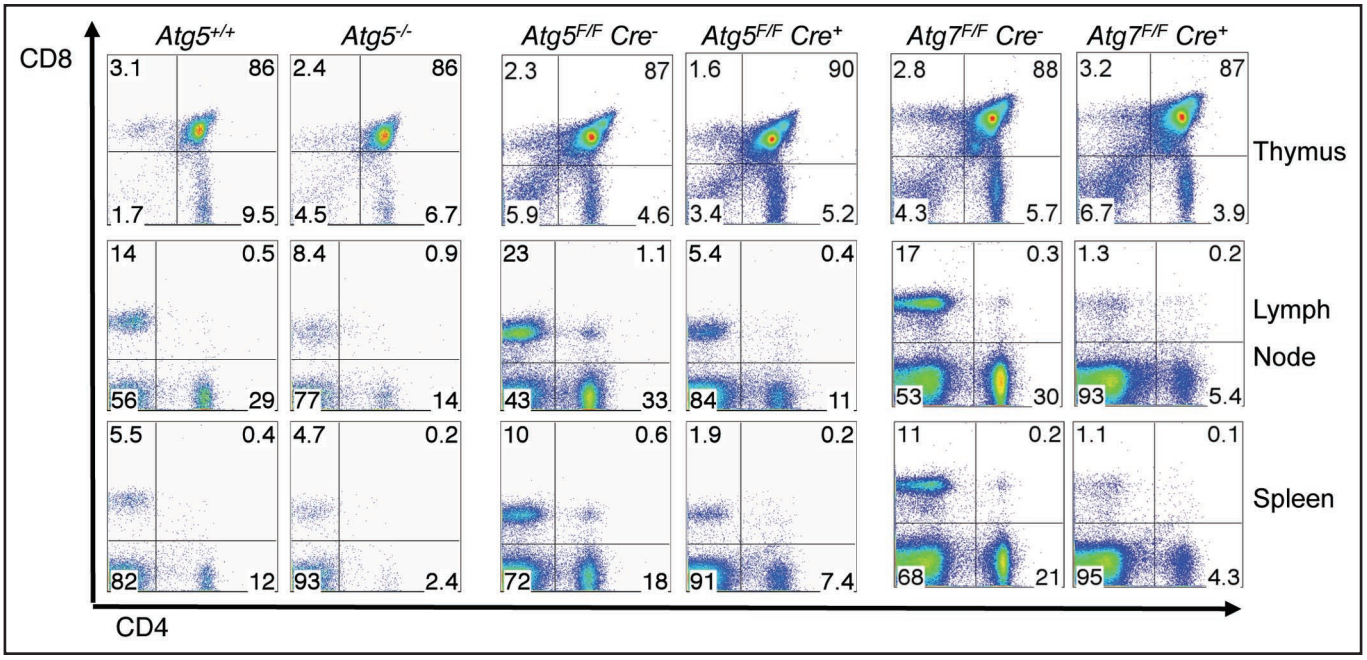

Figure 2. Loss of T cells in *Atg5*$^{-/-}$ chimeric, *Atg5*$^{F/F}$ *Cre*$^{+}$ and *Atg7*$^{F/F}$ *Cre*$^{+}$ mice. Single-cell suspensions of thymocytes, splenocytes and lymph node cells were analyzed by flow cytometry as described in Materials and Methods. Cells were gated by forward and side scatter on lymphocyte populations. Shown is one representative experiment from n ≥ 3 experiments, with at least seven mice of each genotype analyzed.

association between autophagy and mitochondrial maintenance. We identified 64 mitochondrial-associated genes in the *Atg5*-dependent gene set (Fig. 3A) from GO annotation and a recent comprehensive genome-wide survey of genes participating in mitochondrial-associated processes.[34] This *Atg5*-dependent gene set GO signature strongly suggests a role for *Atg5* in mitochondrial function and/or maintenance.

As an additional computational strategy to elucidate potential connections of *Atg5* with mitochondrial function, we projected the *Atg5*-dependent gene set onto human orthologs and generated a human protein-protein interaction (interolog) network (Fig. 3C). The network was built by interrogating data from the HPRD database which contains protein-protein interactions from the literature and from multiple large-scale interactome datasets. We next intersected this network analysis with GO cellular compartment annotations. This approach yielded mitochondrion-anchored subnetworks which we then extended by an additional degree of separation, thereby including non-*Atg5*-dependent gene set proteins that interacted with mitochondrion-associated *Atg5*-dependent gene set-encoded products. We observed that many of these interacting partners are also annotated as mitochondrial related, further supporting the involvement of an enriched subset of *Atg5*-dependent gene set in mitochondrial processes.

We present a diagrammatic summary of the key mitochondrial-associated *Atg5*-dependent genes in Figure 3D, assembled from gene ontology annotations, network data, pathway information and literature (PubMed) co-citation analysis incorporating search terms such as 'mitochondrial biogenesis,' 'mitochondrial permeability' and 'electron transport' (Suppl. Fig. 3A) to gain additional insights into various mitochondrial processes or events in which the *Atg5*-dependent gene set might be involved. We extended this analysis to include other terms associated with various general cellular processes (e.g., endocytosis) and also events specific to T lineage cells and immune function (Suppl. Fig. 3B).

Notably, this analysis revealed described associations in the generation of reactive oxygen species (ROS), lymphocyte activation and lymphocyte proliferation (Suppl. Fig. 3B) in the context of potential functions of *Atg5* in T lineage cells. Consistent with the requirement of *Atg5* in the formation of autophagosomal structures in T cells, our analyses also revealed a connection of *Atg5* with phagocytosis, endocytosis and lysosome formation/function (Suppl. Fig. 3B and ref. 28). Taken together, these transcriptional profiling and computational analyses of orthogonal data, ranging from gene coregulation to protein-protein interaction network with pathway analysis, suggest a role for *Atg5* in mitochondrial maintenance and function.

Survival and proliferation defects in *Atg5*-deficient T cells. Given these transcriptional alterations in *Atg5*-deficient T cells, we further characterized the T cells that develop in the absence of *Atg5*. The expression of the maturation marker CD24 (HSA) was similar between wild-type and *Atg5*-deficient T cells, indicating that peripheral *Atg5*-deficient T cells were phenotypically mature. Strikingly, however, we observed an alteration in the expression of markers associated with activation/memory/homeostatic expansion, CD44 and CD62L (Fig. 4A and B). While the majority of wild-type lymph node and splenic T cells were CD62L^{high} CD44^{low}, *Atg5*-deficient T cells were predominantly CD44^{high} and CD62L^{low}. Peripheral T cells from *Atg7*$^{F/F}$ *Cre*$^{+}$ mice had a similar expression profile for CD44 and CD62L (data not shown). Increased cell surface expression of CD44 and decreased expression

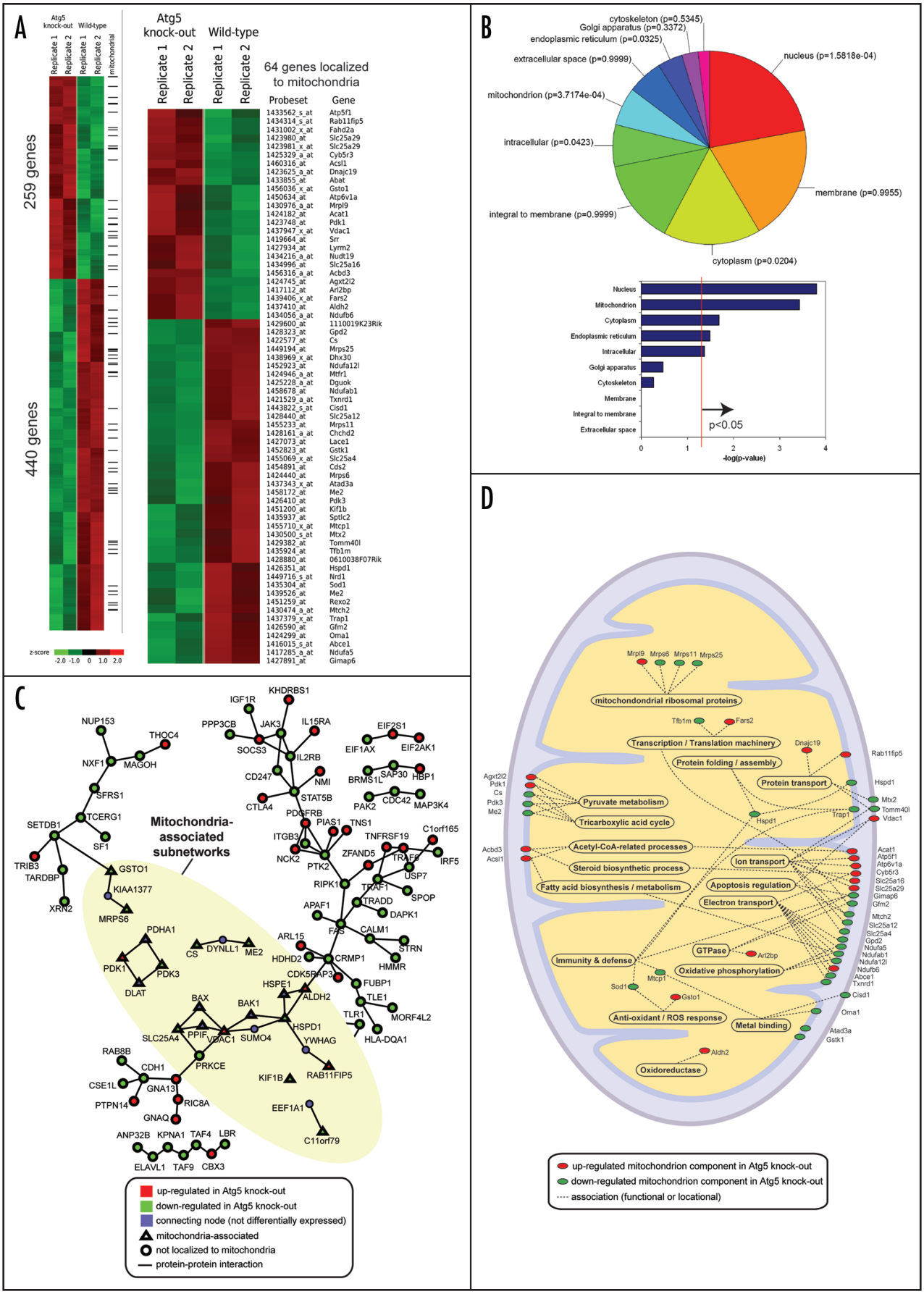
A
Atg5 knock-out
Wild-type
Replicate 1
Replicate 2
Mitochondrial
259 genes
440 genes
z-score
-2.0 -1.0 0 1.0 2.0
64 genes localized to mitochondria
Probeset Gene
1433562_s_at Atp5f1
1434314_s_at Rab11fip5
1431002_x_at Fahd2a
1423980_at Slc25a29
1423981_x_at Slc25a29
1425329_a_at Cyb5r3
1460316_at Acsl1
1423625_a_at Dnajc19
1433855_at Abat
1456036_x_at Gsto1
1450634_at Atp6v1a
1430976_a_at Mrpl9
1424182_at Acat1
1423748_at Pdk1
1437947_x_at Vdac1
1419664_at Srr
1427934_at Lyrm2
1434216_a_at Nudt19
1434996_at Slc25a16
1456316_a_at Acbd3
1424745_at Agxt2l2
1417112_at Arl2bp
1439406_x_at Fars2
1437410_at Aldh2
1434056_a_at Ndufb6
1429600_at 1110019K23Rik
1428323_at Gpd2
1422577_at Cs
1449194_at Mrps25
1438969_x_at Dhx30
1452923_at Ndufa12l
1424946_a_at Mtfr1
1425228_a_at Dguok
1458678_at Ndufab1
1421529_a_at Txnrd1
1443822_s_at Cisd1
1428440_at Slc25a12
1455233_at Mrps11
1428161_a_at Chchd2
1427073_at Lace1
1452823_at Gstk1
1455069_x_at Slc25a4
1454891_at Cds2
1424440_at Mrps6
1437343_x_at Atad3a
1458172_at Me2
1426410_at Pdk3
1451200_at Kif1b
1435937_at Sptlc2
1455710_x_at Mtcp1
1430500_s_at Mtx2
1429382_at Tomm40l
1435924_at Tfb1m
1428880_at 0610038F07Rik
1426351_at Hspd1
1449716_s_at Nrd1
1435304_at Sod1
1439526_at Me2
1451259_at Rexo2
1430474_a_at Mtch2
1437379_x_at Trap1
1426590_at Gfm2
1424299_at Oma1
1416015_s_at Abce1
1417285_a_at Ndufa5
1427891_at Gimap6
B
cytoskeleton (p=0.5345)
Golgi apparatus (p=0.3372)
endoplasmic reticulum (p=0.0325)
extracellular space (p=0.9999)
nucleus (p=1.5818e-04)
mitochondrion (p=3.7174e-04)
intracellular (p=0.0423)
membrane (p=0.9955)
integral to membrane (p=0.9999)
cytoplasm (p=0.0204)
Nucleus
Mitochondrion
Cytoplasm
Endoplasmic reticulum
Intracellular
Golgi apparatus
Cytoskeleton
Membrane
Integral to membrane
Extracellular space
p<0.05
0 1 2 3 4
-log(p-value)
C
Mitochondria-associated subnetworks
NUP153
THOC4
NXF1
MAGOH
SFRS1
SETDB1
TCERG1
SF1
TRIB3
TARDBP
GSTO1
XRN2
KIAA1377
MRPS6
PDHA1
PDK1
PDK3
DLAT
CS
DYNLL1
ME2
BAX
BAK1
PPIF
VDAC1
SUMO4
SLC25A4
HSPD1
YWHAG
RAB8B
CDH1
PRKCE
CSE1L
GNA13
PTPN14
RIC8A
GNAQ
ANP32B
KPNA1
TAF4
LBR
ELAVL1
TAF9
CBX3
KIF1B
RAB11FIP5
EEF1A1
C11orf79
ARL15
HDHD2
CRMP1
CDK5RAP3
HSPE1
ALDH2
FUBP1
TLE1
TLR1
MORF4L2
HLA-DQA1
STRN
HMMR
CALM1
FAS
APAF1
TRADD
DAPK1
RIPK1
TRAF1
SPOP
USP7
ZFAND5
TRAF6
TNFRSF19
C1orf165
IRF5
NCK2
PTK2
ITGB3
PDGFRB
PIAS1
TNS1
STAT5B
CTLA4
NMI
CD247
IL2RB
SOCS3
JAK3
PPP3CB
IL15RA
IGF1R
KHDRBS1
EIF1AX
EIF2AK1
EIF2S1
BRMS1L
SAP30
HBP1
PAK2
CDC42
MAP3K4
up-regulated in Atg5 knock-out
down-regulated in Atg5 knock-out
connecting node (not differentially expressed)
mitochondria-associated
not localized to mitochondria
protein-protein interaction
D
Mrpl9 Mrps6 Mrps11 Mrps25
mitochondrial ribosomal proteins
Tfb1m
Fars2
Transcription / Translation machinery
Dnajc19
Rab11fip5
Protein folding / assembly
Protein transport
Hspd1
Agxt2l2
Pdk1
Cs
Pdk3
Me2
Pyruvate metabolism
Tricarboxylic acid cycle
Hspd1
Trap1
Mtx2
Tomm40l
Vdac1
Acbd3
Acsl1
Acetyl-CoA-related processes
Steroid biosynthetic process
Fatty acid biosynthesis / metabolism
Ion transport
Apoptosis regulation
Electron transport
Acat1
Atp5f1
Atp6v1a
Cyb5r3
Slc25a16
Slc25a29
Gimap6
Gfm2
Mtch2
Slc25a12
Slc25a4
Gpd2
Ndufa5
Ndufab1
Ndufa12l
Ndufb6
Abce1
Txnrd1
Cisd1
Oma1
Atad3a
Gstk1
Immunity & defense
GTPase
Arl2bp
Oxidative phosphorylation
Mtcp1
Sod1
Gsto1
Anti-oxidant / ROS response
Metal binding
Aldh2
Oxidoreductase
up-regulated mitochondrion component in Atg5 knock-out
down-regulated mitochondrion component in Atg5 knock-out
association (functional or locational)

Figure 3. (See previous page). *Atg5* is required for the proper regulation of mitochondrial-associated gene sets. (A) Microarray analysis showing genes differentially expressed ($p < 0.05$), of which 259 genes were induced and 440 downregulated in *Atg5*$^{-/-}$ thymocytes compared to wild-type thymocytes. Expression values for each probeset were z-score-transformed across all arrays and their intensities above and below the mean are represented on the heatmap by red and green colors respectively, as shown on the color bar. Genes were hierarchically clustered using Cluster 3.0 and visualized with Java TreeView. Tick markings highlight 64 differentially expressed mitochondrial genes, whose expression profiles are displayed by the heatmap on the right. (B) Differentially expressed genes were classified into gene ontology (GO) cellular component categories. Categories assigned with at least 3 genes are displayed as a pie chart, with enrichment p-values shown in brackets alongside each category. The bar chart displays enrichment p-values as negative log-transformed values, which reveals a dramatic enrichment of mitochondria- and nucleus-associated genes. (C) Construction of human protein-protein interaction (interolog) network. Differentially expressed genes were mapped onto human orthologs for which interaction data was available. Circles representing upregulated components are colored red and downregulated components green. Solid lines denote protein-protein interactions. Mitochondrion-anchored subnetworks (highlighted by the yellow region) emerged when extending connections by an additional degree of separation, capturing components of interest (blue circles) in the functional neighborhood of mitochondrial-related genes that were found to be differentially expressed. Network clusters containing connections between at least 3 components are displayed. (D) Diagrammatic mitochondrion representation showing key differentially expressed gene products participating in mitochondria-associated processes. Red and green ovals denote differentially up and downregulated components respectively. Functional associations with biological processes are represented by dashed lines.

of CD62L have been reported in T cells undergoing homeostatic expansion.[35-39] Importantly, expression levels of T cell antigen receptor did not appear altered in the *Atg5*-deficient T cells, nor were there significant differences in the expression of the early activation markers CD25 and CD69 (Fig. 4A), consistent with the hypothesis that *Atg5*-deficient T cells may be responding to homeostatic rather than antigen-induced expansion signals.[40]

T cells in lymphopenic mice undergo multiple rounds of proliferation in order to reach peripheral homeostasis.[41] The decreased number of peripheral T cells together with a surface phenotype indicative of homeostatic expansion suggest that *Atg5*-deficient T cells may be unable to populate the peripheral lymphoid organs, possibly due to survival defects, resulting in a compensatory proliferative response. Consistent with this view, we found that freshly isolated T cells from *Atg5*$^{-/-}$ chimeras contained a significant proportion of cells undergoing death as indicated by Annexin-V staining among both the CD62L^{low} and CD62L^{high} populations. Compared to wild-type cells, the proportion of Annexin-V^{+} cells was 1.5- to 2-fold higher in CD62L^{low} *Atg5*-deficient T cells, and 3- to 7-fold higher in CD62L^{high} *Atg5*-deficient T cells (Fig. 4C). Annexin-V staining was also elevated in CD62L^{high} populations of *Atg5*$^{F/F}$ *Cre*$^{+}$ T cells (Fig. 4D). These data indicate the requirement for *Atg5* in the survival of T lymphocytes.

Consistent with the results of Pua et al.[11] *Atg5*-deficient T cells exhibited a severe defect in TCR-induced proliferation (Fig. 5). We purified CD62L^{high} T lymphocytes from control and *Atg5*$^{-/-}$ chimeras, labeled them with CFSE, stimulated them with anti-CD3 and anti-CD28 antibodies, and analyzed proliferation at 72 hours. We also measured blast formation using T cells stimulated with anti-CD3 and anti-CD28 antibodies for 40 hours. We observed a severe reduction in proliferation and the ability to form blasts in *Atg5*-deficient T cell cultures compared to controls (Fig. 5). We conclude that *Atg5* is important for T cell survival and proliferation after antigen receptor stimulation.

Increased mitochondrial mass in *Atg5*-deficient T lymphocytes. Our transcriptional profiling analyses of *Atg5*-deficient T cells raised the possibility that the defects in T cell homeostasis observed in the absence of *Atg5* are due to impaired mitochondrial function. To determine if mitochondria were normal in the absence of *Atg5*, we analyzed mitochondrial mass/volume in single cells using the vital dye Mitotracker green, a mitochondrial specific dye. We observed an increase in Mitotracker staining in *Atg5*-deficient splenic CD4^{+} and CD8^{+} T cells from both *Atg5*$^{-/-}$ chimeric and *Atg5*$^{F/F}$ *Cre*$^{+}$ mice relative to controls (Fig. 6A and data not shown). The Mitotracker staining of thymocytes from *Atg5*$^{-/-}$ chimeras was similar to wild-type cells, suggesting that the increase in mitochondrial mass occurred as the T cells aged (data not shown).

We next asked if alterations in mitochondrial mass correlated with the decrease in cell survival in *Atg5*-deficient T cells. We costained splenocytes from *Atg5*$^{F/F}$ *Cre*$^{+}$ and *Atg5*$^{F/F}$ *Cre*$^{-}$ mice with Mitotracker green and Annexin-V. CD4^{+} and CD8^{+} T cells that were Mitotracker^{high} had a significantly higher percentage of cells that were Annexin-V^{+} compared with Mitotracker^{low} T cells (Fig. 6B). Although this trend was apparent in both *Atg5*$^{F/F}$ *Cre*$^{+}$ and *Atg5*$^{F/F}$ *Cre*$^{-}$ mice, there was an increase of approximately 15% in the percentage of Annexin-V^{+} cells within the Mitotracker^{high} population in *Atg5*$^{F/F}$ *Cre*$^{+}$ mice (Fig. 6B). These data show that mitochondrial mass correlates with Annexin-V staining in CD4^{+} and CD8^{+} T cells, suggesting that the increase in mitochondrial mass in *Atg5*-deficient T cells correlates with increased death in these cells.

Discussion

Our data suggests that autophagy is an active process during all stages of T lymphocyte development and that deletion of the essential autophagy genes, *Atg5* and *Atg7*, results in profound abnormalities in T cell maintenance. In addition, we showed that *Atg5* is important for T cell survival. Transcriptional profiling of *Atg5*-deficient thymocytes suggests abnormalities in mitochondria in the absence of this autophagy gene. This hypothesis is supported by studies indicating that there is an increase in mitochondrial mass in peripheral *Atg5*-deficient T cells. Mitochondrial mass is correlated with Annexin-V staining of peripheral T cells, suggesting a link between mitochondrial abnormalities and *Atg5*-deficient T cell death. Given our gene chip and mitochondrial mass results, we propose that autophagy is required in T lymphocytes for normal mitochondrial maintenance.

Although dramatic mitochondria-related transcriptional changes were observed in thymocytes, we did not observe an increase in mitochondrial mass in *Atg5*-deficient thymocytes, but only in peripheral *Atg5*-deficient T cells. Despite the two-fold decrease in thymus cellularity in *Atg5*$^{-/-}$ chimeras, we also did not observe an increase in Annexin-V staining in the thymus, consistent

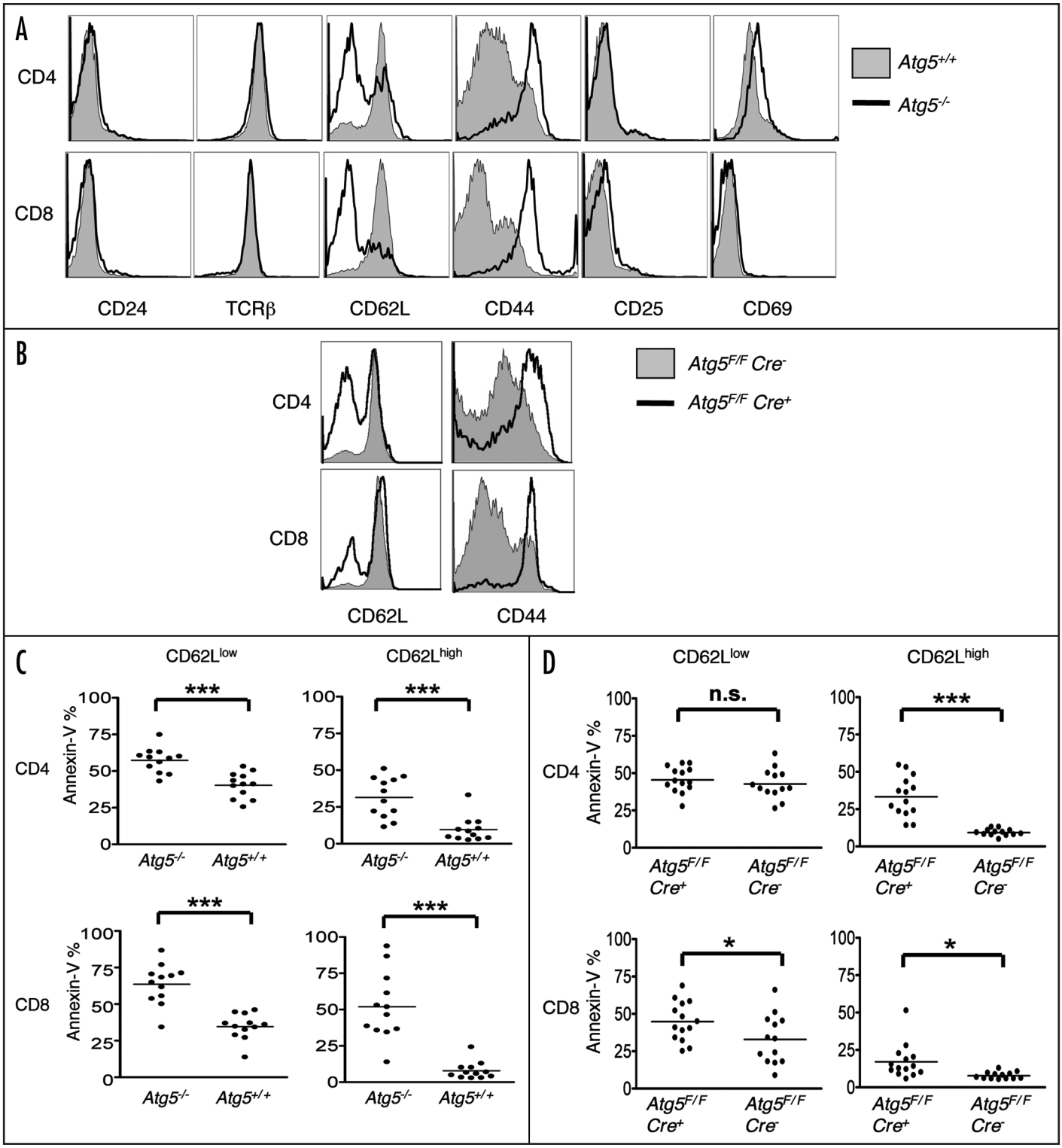

Figure 4. A higher percentage of T cells are CD44 ^{high}, CD62L^{low} and Annexin-V^{+} in *Atg5*$^{-/-}$ chimeras and *Atg5*$^{F/F}$ *Cre*$^{+}$ mice compared with controls. (A and B) Flow cytometric analysis of lymph node T lymphocytes from *Atg5*$^{+/+}$ or *Atg5*$^{-/-}$ chimeric mice (A) or *Atg5*$^{F/F}$ Cre^{-} and *Atg5*$^{F/F}$ Cre^{+} mice (B). Cells were gated by forward and side scatter for lymphocytes, then gated on CD4^{+} or CD8^{+} cells. One representative experiment shown of at least five independent experiments. C-D. Lymph node T cells from *Atg5*$^{+/+}$ or *Atg5*$^{-/-}$ chimeric mice (C) or *Atg5*$^{F/F}$ Cre^{-} or *Atg5*$^{F/F}$ Cre^{+} mice (D) were stained with Annexin-V and antibodies against CD4, CD8 and CD62L. Cells were gated by forward and side scatter for lymphocytes, then gated on CD4^{+} or CD8^{+} cells. Data pooled from at least four independent experiments. (*$p < 0.05$, **$p < 0.005$, ***$p < 0.0005$, n.s. = not statistically significant).

with a previous report.[11] We hypothesize that we are unable to detect mitochondrial abnormalities because the cells have not yet accumulated sufficient damaged mitochondria to die. Alternatively, the actively phagocytic cells of the thymus responsible for the normal elimination of thymocytes that have failed the selection process[42] may be quickly removing those *Atg5*-deficient thymocytes that have accumulated damaged mitochondria. It is interesting that the transcriptional signature observed here for *Atg5*-deficient thymocytes is quite distinct from the signature observed in either Paneth cells or thymocytes cells that express lower than normal levels of ATG16L1.[43] This suggests that the transcriptional response to autophagy gene-deficiency may differ depending on the primary cell type involved. This is important since it may explain potential differences in the role of autophagy genes in closely related cells.[12]

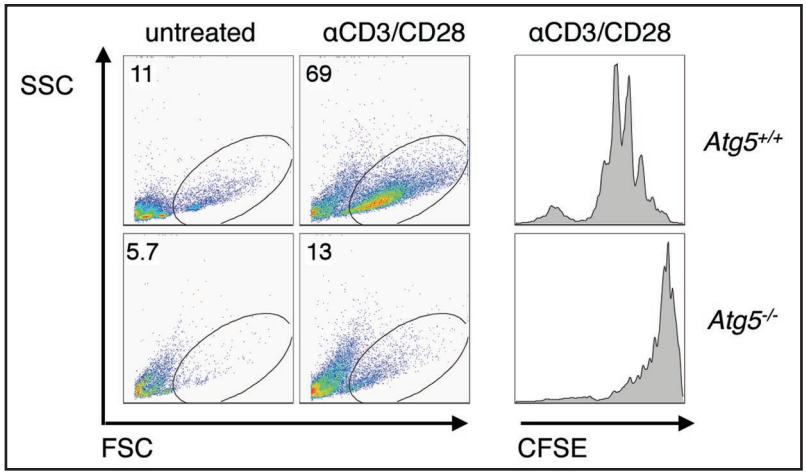

Figure 5. Proliferation defect in *Atg5*-deficient T lymphocytes. Purified CD62L^{high} T cells from *Atg5*$^{+/+}$ or *Atg5*$^{-/-}$ chimeric mice were either untreated or stimulated with anti-CD3 (1 μg/mL) and anti-CD28 (1 μg/mL) and analyzed 40 hours later for T cell blasts (left panels) or loaded with CFSE, stimulated as above, and analyzed 72 hours later (right panel). Shown is one representative experiment of three. CD4^{+} cells shown.

We utilized three different approaches in this study to address the importance of autophagy genes in T lineage cells. In the first approach, *Rag1*$^{-/-}$ complementation, analysis of *Atg5*$^{-/-}$ T cells is potentially complicated due to the decrease in viability of *Atg5*$^{-/-}$ chimeras and the deletion of *Atg5* in other hematopoietic cell types in addition to T cells, resulting in defects in other cell lineages.[12] By using a conditional knockout approach we ascertained that *Atg5* is required within T cells for their maintenance in vivo. Our western blot results suggest that deletion of the *Atg5*^{flox} alleles may be incomplete in some cells or that the ATG5 protein may be retained for a significant time after gene deletion. Despite these caveats, given that the in vivo phenotypes of *Atg5*$^{-/-}$, *Atg5*$^{F/F}$ *Cre*$^{+}$ and *Atg7*$^{F/F}$ *Cre*$^{+}$ T cells are similar, it is likely that these phenotypes are due to the lack of autophagy in T cells, and not due to nonautophagy functions of *Atg5*[27] or *Atg7*. However, since ATG7 is essential for the conjugation of ATG5 to ATG12,[4,44] it is possible that a nonautophagy role of the ATG5-12 conjugate is responsible. Further studies will be necessary to distinguish between these possibilities.

Materials and Methods

Mice and cells. The generation of *Atg5*$^{-/-}$, *Atg5*$^{F/F}$ and *Atg7*$^{F/F}$ mice has been previously described.[6,7,26] Chimeric mice were generated by reconstituting sublethally irradiated B6.129S7-*Rag1*^{tm1Mom}/J (*Rag1*$^{-/-}$, The Jackson Laboratory, #002216) mice with *Atg5*$^{+/+}$ or *Atg5*$^{-/-}$ fetal liver cells, as previously described.[12] *Atg5*$^{F/F}$ and *Atg7*$^{F/F}$ were bred to lck-*Cre* (C57BL/6NTac-TgN(Lck-Cre)) transgenic mice (Taconic, #004197, Hudson, New York). Mice were maintained at Washington University School of Medicine in accordance with institutional policies for animal care and usage. *Atg5*$^{-/-}$ and *Atg5*$^{+/+}$ embryonic fibroblasts were generated from day 13.5 embryos. To establish immortalized cell lines, 10^6 cells were transformed with 1ug of pEF321-T, an SV40 large T antigen expression vector (a gift from T. Hansen), by the FuGENE HD transfection reagent (Roche, Basel, Switzerland) according to the manufacturer's instructions.

Genotyping. Genotyping of the mice was performed as described,[7,26] with the *Cre* gene detected with primers cre1 (AGG TTC GTT CAC TCA TGG A) and cre2 (TCG ACC AGT TTA GTT ACC C) using PCR [94°C (4 min); 25 cycles of 94°C (30 sec), 60°C (30 sec), 72°C (1 min); 72°C (5 min)]. The *Atg5* gene was detected with the primers exon3-1 (GAA TAT GAA GGC ACA CCC CTG AAA TG), short2 (GTA CTG CAT AAT GGT TTA ACT CTT GC), and check2 (ACA ACG TCG AGC ACA GCT GCG CAA GG) using PCR [94°C (4 min); 30 cycles of 94°C (30 sec), 60°C (30 sec), 72°C (1 min); 72°C (5 min)]. The same PCR program was used with the primers short2, check2 and 5L2 (CAG GGA ATG GTG TCT CCC AC) to check for the *Atg5*^{flox} and deleted *Atg5*^{flox} alleles in thymocytes from *Atg5*$^{F/F}$ *Cre*$^{+}$ and *Atg5*$^{F/F}$ *Cre*$^{-}$ mice. The *Atg7*^{flox} gene was detected with primers Hind-Fw (TGG CTG CTA CTT CTG CAA TGA TGT) and Pst-Rv (CAG GAC AGA GAC CAT CAG CTC CAC) using PCR [94°C (5 min); 30 cycles of 94°C (20 sec), 68°C (30 sec), 72°C (90 sec); 72°C (10 min)]. Confirmation of the wild-type *Atg7* locus was done with primers Ex14 F (TCT CCC AAG ACA AGA CAG GGT GAA) and Ex14 R (AAG CCA AAG GAA ACC AAG GGA GTG) using PCR [94°C (5 min); 35 cycles of 94°C (20 sec), 60°C (15 sec), 72°C (60 sec); 72°C (10 min)].

Stimulation and proliferation assays. Single cell suspensions from the spleens and lymph nodes of chimeric mice were first B cell depleted using negative selection with anti-B220-Dynal beads (Invitrogen, Carlsbad, California), followed by positive selection for CD62L^{high} lymphocytes. Briefly, cells were incubated with biotin-conjugated anti-CD62L antibody (Caltag, Carlsbad, California) followed by antibiotin MACs beads (Miltenyi Biotec, Auburn, California) and isolated according to the manufacturer's instructions. CD62L^{high} purities were greater than 90%. T cells were plated at 1 x 10^6/mL in complete media (DMEM (Gibco, Carlsbad, California) plus 10% fetal calf serum (FCS), 100 Units/mL penicillin, 100 ug/mL streptomycin, 1 mM sodium pyruvate, 2 mM L-glutamine, 1x non-essential amino acids (Gibco, Carlsbad, California) and 57 uM β-mercaptoethanol). Cells were stimulated with 1.0 μg/mL anti-CD3 and 1.0 μg/mL anti-CD28

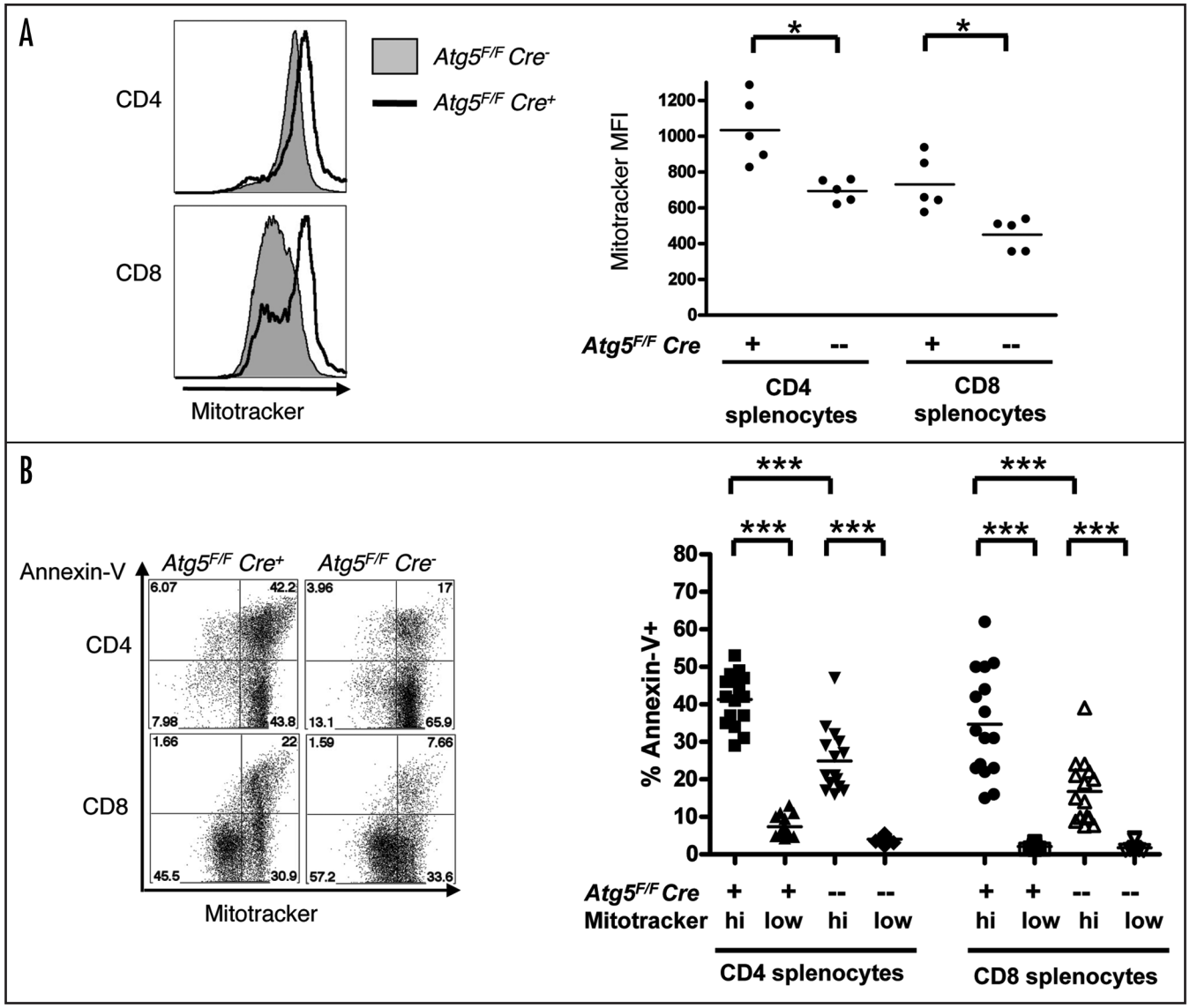

Figure 6. *Atg5*-deficient T lymphocytes have an increase in mitochondrial mass. (A) Splenocytes from $Atg5^{F/F}$ Cre^{+} and $Atg5^{F/F}$ Cre^{-} mice were loaded with MitoTracker green, stained with antibodies against CD4 or CD8, and analyzed by flow cytometry. Analysis was performed on $CD4^{+}$ or $CD8^{+}$ splenocytes without gating by forward and side scatter. Shown are representative FACS plots of at least fifteen mice of each genotype and the quantation of the mean fluorescence intensity (MFI) of Mitotracker staining from one of three independent experiments. (B) Splenocytes from $Atg5^{F/F}$ Cre^{+} and $Atg5^{F/F}$ Cre^{-} mice were stained with CD4, CD8, Mitotracker green, and Annexin-V. Representative FACS plots and quantitation of the percentage of Annexin-V^{+} cells from the $Mitotracker^{high}$ and $Mitotracker^{low}$ gates are shown. Analysis was performed on $CD4^{+}$ or $CD8^{+}$ splenocytes without gating by forward and side scatter. Data pooled from three independent experiments. (*$p < 0.05$, **$p < 0.005$, ***$p < 0.0005$, n.s. = not statistically significant).

(BD Biosciences, San Jose, California). To label cells with CFSE, cells were incubated with 1 μM CFSE (Invitrogen, Carlsbad, California) for 30 minutes at 37°C and then washed in complete media. Labeled cells were cultured with the indicated stimuli for 72 hours and then analyzed by flow cytometry.

Flow cytometry and cell sorting. Single cell suspensions were prepared from the spleens, thymus, and lymph nodes and stained with antibodies recognizing TCRβ, CD4, CD8, CD24, CD25, CD44, CD62L and CD69 (BD Biosciences, San Jose, California). Annexin-V labeling was performed by surface staining cells with the indicated lineage markers, washing with complete media, and staining for 15 minutes with Annexin-V (BD Biosciences, San Jose, California). Thymocytes were sorted on a FACS Vantage SE (BD Biosciences, San Jose, California) by FSC/SSC gating on a live lymphocyte population, followed by gating out $CD11b^{+}$, $CD11c^{+}$ and $B220^{+}$ cells. The remaining cells were then sorted based on expression of CD4 and CD8. Purities were greater than 94% for each population (n = 4 independent experiments). Peripheral $CD4^{+}$ and $CD8^{+}$ T cells were isolated using negative selection by MACS magnetic bead sorting according to the manufacturer's instructions (Miltenyi Biotec, Auburn, California). Peripheral T cells were negatively selected from pooled spleen and lymph node samples, followed by negative selection against either $CD4^{+}$ or $CD8^{+}$ cells. Purities averaged

86% for CD4+ cells and 92% for CD8+ cells (n = 4 independent experiments).

Statistics. All non-gene chip data were analyzed with Prism software (Graphpad; San Diego, California), using two-tailed unpaired Student's t tests.

Western blotting. Cells were washed with PBS and then lysed in cold NP-40 lysis buffer [0.5% NP-40, 50 mM Tris-Cl, 150 mM NaCl, 1 mM EDTA, 1 mM phenylmethylsulfonyl fluoride] or cold lysis buffer B [50 mM Tris-HCl pH 8.0, 150 mM NaCl, 1% Triton X-100, 0.1% SDS, 0.2% deoxycholic acid sodium salt] supplemented with complete pretease inhibitors (Roche, Basel, Switzerland) for 10 minutes at 4°C. Lysates were cleared by centrifugation at 14,000 x g for 10 minutes at 4°C. Samples were analyzed by western blotting[12] using antibodies against ATG5 (Novus Biologicals, Littleton, Colorado, and Nanotools, Teningen, Germany), ATG7 (Sigma, St. Louis, Missouri), LC3 (Novus Biologicals, Littleton, Colorado) and β-actin (Sigma, St. Louis, Missouri).

Mitochondria mass/volume assay. Cells were loaded with 100 nM MitoTracker Green (Invitrogen, Carlsbad, California) for 30 minutes at 37°C in the presence of flourochome-conjugated antibodies against CD4 and CD8. Cells were washed and then analyzed by flow cytometry. When necessary, Annexin-V was added after washing the cells in complete media.

Microarrays and analysis. Total thymocyte RNA was harvested from *Atg5*$^{-/-}$ and *Atg5*$^{+/+}$ chimeras by lysing single cell suspensions of thymocytes in Trizol (Invitrogen, Carlsbad, California). RNA analyses were performed at the microarray core facility at the Harvard Medical School and Partners Healthcare Center for Genetics and Genomics. The quantity, purity and integrity of RNA were evaluated by UV spectrophotometry and RNA-nano Bioanalyzer (Agilent, Santa Clara, California). Sample processing and hybridization on Mouse Genome 430 2.0 GeneChip microarrays (Affymetrix, Santa Clara, California) were performed according to manufacturer's instructions. Probe-level normalization of the raw CEL data files using the GC Robust Multi-array Average (GCRMA) algorithm[45] was implemented in the R programming language. Two-sided t-test was performed for each probeset, comparing between *Atg5*$^{-/-}$ and *Atg5*$^{+/+}$ chimera samples. Probesets with $p < 0.05$ were considered differentially expressed. Hierarchical clustering (pairwise complete-linkage) of probesets corresponding to differentially expressed genes was performed with Cluster 3.0,[46] using the Pearson's correlation coefficient as the similarity metric. Z-score transformation was applied to each probeset across all arrays prior to generating 'heatmaps' for visualization implemented in the Python language.

Gene ontology (GO) analysis. Differentially expressed genes were examined in terms of GO cellular component categories.[30] To assess enrichment of these categories within the set of differentially expressed genes against all genes represented by probes on the Affymetrix Mouse Genome 430 2.0 microarray GeneChip, p-values were computed using Fisher's exact test implemented in Python and R programming languages. Categories with $p < 0.05$ were considered significantly enriched.

Protein interaction network. The network was constructed by iteratively connecting interacting proteins, with data extracted from a collection of genome-wide interactome screens and curated literature entries in HPRD.[31] The network uses graph theoretic representations, which abstract components (gene products) as nodes and relationships (e.g., interactions) between components as edges, implemented in the Perl programming language.

Literature co-citation analysis. Co-citation analysis was performed using Milano search,[33] identifying the number of times a gene was co-cited with a specified term in articles from the PubMed database. Vectors capturing the co-citation profiles for each of these genes were generated for a set of terms and clustered using pairwise complete-linkage hierarchical clustering with the Pearson's correlation coefficient as the similarity measure. The results were displayed as a heatmap implemented in the Python language.

Acknowledgements

Financial support for this work was provided by NIH grants P30-AR048335 and R01-AI061077 (W.S.), CA74730 and U54A1057160 (H.W.V), R01-AI062773 and R01-DK83756 (R.X.), 5-T32-AI07163-27 (L.M.S.), Grants-in-Aid for Scientific Research from the Ministry of Education, Culture, Sports, Science and Technology, Japan, and the Toray Science Foundation (N.M). A. N. is a recipient of a fellowship award from the Crohn's and Colitis Foundation of America. K.C. is the Lallage Feazel Wall Fellow of the Damon Runyon Cancer Research Foundation, DRG-1972-08.

We thank David Strong and Boris Calderon for assistance with the generation of chimeric mice. We also thank Suzanne Schloemann of the Department of Pathology and Immunology's Flow Cytometry Center for assistance with cell sorting. We thank Heather H. Pua and You-Wen He for the *Atg7* wild-type genotyping protocol.

Note

Supplementary materials can be found at:
www.landesbioscience.com/supplement/StephensonAUTO5-5-Sup.pdf

References

1. Levine B and Kroemer G. Autophagy in the Pathogenesis of Disease. Cell 2008; 132:27-42.
2. Mizushima N, Levine B, Cuervo AM and Klionsky DJ. Autophagy fights disease through cellular self-digestion. Nature 2008; 451:1069-75.
3. Kroemer G and Levine B. Autophagic cell death: the story of a misnomer. Nat Rev Mol Cell Biol 2008; 9:1004-10.
4. Mizushima N, Ohsumi Y and Yoshimori T. Autophagosome formation in mammalian cells. Cell Struct Funct 2002; 27:421-9.
5. Hanada T, Noda NN, Satomi Y, Ichimura Y, Fujioka Y, Takao T, et al. The ATG12-ATG5 conjugate has a novel e3-like activity for protein lipidation in autophagy. J Biol Chem 2007.
6. Kuma A, Hatano M, Matsui M, Yamamoto A, Nakaya H, Yoshimori T, et al. The role of autophagy during the early neonatal starvation period. Nature 2004; 432:1032-6.
7. Komatsu M, Waguri S, Ueno T, Iwata J, Murata S, Tanida I, et al. Impairment of starvation-induced and constitutive autophagy in Atg7-deficient mice. J Cell Biol 2005; 169:425-34.
8. Li C, Capan E, Zhao Y, Zhao J, Stolz D, Watkins SC, et al. Autophagy is induced in CD4+ T cells and important for the growth factor-withdrawal cell death. J Immunol 2006; 177:5163-8.
9. Bell BD, Leverrier S, Weist BM, Newton RH, Arechiga AF, Luhrs KA, et al. FADD and caspase-8 control the outcome of autophagic signaling in proliferating T cells. Proc Natl Acad Sci USA 2008; 105:16677-82.
10. Feng CG, Zheng L, Jankovic D, Bafica A, Cannons JL, Watford WT, et al. The immunity-related GTPase Irgm1 promotes the expansion of activated CD4+ T cell populations by preventing interferon-gamma-induced cell death. Nat Immunol 2008; 9:1279-87.
11. Pua HH, Dzhagalov I, Chuck M, Mizushima N and He YW. A critical role for the autophagy gene Atg5 in T cell survival and proliferation. J Exp Med 2007; 204:25-31.

12. Miller BC, Zhao Z, Stephenson LM, Cadwell K, Pua HH, Lee HK, et al. The autophagy gene ATG5 plays an essential role in B lymphocyte development. Autophagy 2007; 4.
13. Nedjic J, Aichinger M, Emmerich J, Mizushima N and Klein L. Autophagy in thymic epithelium shapes the T-cell repertoire and is essential for tolerance. Nature 2008; 455:396-400.
14. Bellu AR, Komori M, van dK I, Kiel JA and Veenhuis M. Peroxisome biogenesis and selective degradation converge at Pex14p. J Biol Chem 2001; 276:44570-4.
15. Kissova I, Deffieu M, Manon S and Camougrand N. Uth1p is involved in the autophagic degradation of mitochondria. J Biol Chem 2004; 279:39068-74.
16. Zhang Y, Qi H, Taylor R, Xu W, Liu LF and Jin S. The role of autophagy in mitochondria maintenance: characterization of mitochondrial functions in autophagy-deficient *S. cerevisiae* strains. Autophagy 2007; 3:337-46.
17. Ebato C, Uchida T, Arakawa M, Komatsu M, Ueno T, Komiya K, et al. Autophagy is important in islet homeostasis and compensatory increase of Beta cell mass in response to high-fat diet. Cell Metab 2008; 8:325-32.
18. Tal MC, Sasai M, Lee HK, Yordy B, Shadel GS and Iwasaki A. Absence of autophagy results in reactive oxygen species-dependent aplification of RLR signaling. Proc Natl Acad Sci USA 2008; In Press.
19. Wang Y, Singh R, Massey AC, Kane SS, Kaushik S, Grant T, et al. Loss of macroautophagy promotes or prevents fibroblast apoptosis depending on the death stimulus. J Biol Chem 2008; 283:4766-77.
20. Zhang H, Bosch-Marce M, Shimoda LA, Tan YS, Baek JH, Wesley JB, et al. Mitochondrial autophagy is an HIF-1-dependent adaptive metabolic response to hypoxia. J Biol Chem 2008; 283:10892-903.
21. Rodriguez-Enriquez S, Kim I, Currin RT and Lemasters JJ. Tracker dyes to probe mitochondrial autophagy (mitophagy) in rat hepatocytes. Autophagy 2006; 2:39-46.
22. Elmore SP, Qian T, Grissom SF and Lemasters JJ. The mitochondrial permeability transition initiates autophagy in rat hepatocytes. FASEB J 2001; 15:2286-7.
23. Shintani T and Klionsky DJ. Autophagy in health and disease: a double-edged sword. Science 2004; 306:990-5.
24. Klionsky DJ, Abeliovich H, Agostinis P, Agrawal DK, Aliev G, Askew DS, et al. Guidelines for the use and interpretation of assays for monitoring autophagy in higher eukaryotes. Autophagy 2008; 4:151-75.
25. Stephenson LM, Sammut B, Graham DB, Chan-Wang J, Brim KL, Huett AS, et al. DLGH1 is a negative regulator of T-lymphocyte proliferation. Mol Cell Biol 2007; 27:7574-81.
26. Hara T, Nakamura K, Matsui M, Yamamoto A, Nakahara Y, Suzuki-Migishima R, et al. Suppression of basal autophagy in neural cells causes neurodegenerative disease in mice. Nature 2006; 441:885-9.
27. Codogno P and Meijer AJ. Atg5: more than an autophagy factor. Nat Cell Biol 2006; 8:1045-7.
28. Sanjuan MA, Dillon CP, Tait SW, Moshiach S, Dorsey F, Connell S, et al. Toll-like receptor signaling in macrophages links the autophagy pathway to phagocytosis. Nature 2007; 450:1253-7.
29. Zhao Z, Fux B, Goodwin M, Dunay IR, Strong D, Miller BC, et al. Autophagosome-independent essential function for the autophagy protein Atg5 in cellular immunity to intracellular pathogens. Cell Host Microbe 2008; 4:458-69.
30. The Gene Ontology project in 2008. Nucleic Acids Res 2008; 36:440-4.
31. Mishra GR, Suresh M, Kumaran K, Kannabiran N, Suresh S, Bala P, et al. Human protein reference database—2006 update. Nucleic Acids Res 2006; 34:411-4.
32. Wheeler DL, Barrett T, Benson DA, Bryant SH, Canese K, Chetvernin V, et al. Database resources of the National Center for Biotechnology Information. Nucleic Acids Res 2008; 36:13-21.
33. Rubinstein R and Simon I. MILANO—custom annotation of microarray results using automatic literature searches. BMC Bioinformatics 2005; 6:12.
34. Calvo S, Jain M, Xie X, Sheth SA, Chang B, Goldberger OA, et al. Systematic identification of human mitochondrial disease genes through integrative genomics. Nat Genet 2006; 38:576-82.
35. Clarke SR and Rudensky AY. Survival and homeostatic proliferation of naive peripheral CD4$^+$ T cells in the absence of self peptide:MHC complexes. J Immunol 2000; 165:2458-64.
36. Ploix C, Lo D and Carson MJ. A ligand for the chemokine receptor CCR7 can influence the homeostatic proliferation of CD4 T cells and progression of autoimmunity. J Immunol 2001; 167:6724-30.
37. Gudmundsdottir H and Turka LA. A closer look at homeostatic proliferation of CD4$^+$ T cells: costimulatory requirements and role in memory formation. J Immunol 2001; 167:3699-707.
38. Goldrath AW, Bogatzki LY and Bevan MJ. Naive T cells transiently acquire a memory-like phenotype during homeostasis-driven proliferation. J Exp Med 2000; 192:557-64.
39. Murali-Krishna K and Ahmed R. Cutting edge: naive T cells masquerading as memory cells. J Immunol 2000; 165:1733-7.
40. Taylor DK, Neujahr D and Turka LA. Heterologous immunity and homeostatic proliferation as barriers to tolerance. Curr Opin Immunol 2004; 16:558-64.
41. Marrack P, Bender J, Hildeman D, Jordan M, Mitchell T, Murakami M, et al. Homeostasis of alpha beta TCR$^+$ T cells. Nat Immunol 2000; 1:107-11.
42. Surh CD and Sprent J. T-cell apoptosis detected in situ during positive and negative selection in the thymus. Nature 1994; 372:100-3.
43. Cadwell K, Liu JY, Brown SL, Miyoshi H, Loh J, Lennerz JK, et al. A key role for autophagy and the autophagy gene Atg16l1 in mouse and human intestinal Paneth cells. Nature 2008; 456:259-63.
44. Komatsu M, Waguri S, Chiba T, Murata S, Iwata J, Tanida I, et al. Loss of autophagy in the central nervous system causes neurodegeneration in mice. Nature 2006; 441:880-4.
45. Wu Z, Irizarry RA, Gentleman FM, Martinez-Murillo F and Spencer F. A model-based background adjustment for oligonucleotide expression arrays. J Am Stat Assoc 2004; 99:909-18.
46. Eisen MB, Spellman PT, Brown PO and Botstein D. Cluster analysis and display of genome-wide expression patterns. Proc Natl Acad Sci USA 1998; 95:14863-8.